



BIOMEDICAL SCIENCES

Synthesis of 4-(4-chlorophenyl)thiazole compounds: *in silico* and *in vitro* evaluations as leishmanicidal and trypanocidal agents

IRANILDO JOSÉ DA CRUZ FILHO, JAMERSON F. DE OLIVEIRA, ALINE CAROLINE S. SANTOS, VALÉRIA R.A. PEREIRA & MARIA CARMO A. DE LIMA

Abstract: Neglected tropical diseases are a diverse group of communicable pathologies that mainly prevail in tropical and subtropical regions. Thus, the objective of this work was to evaluate the biological potential of eight 4-(4-chlorophenyl)thiazole compounds. Tests were carried out *in silico* to evaluate the pharmacokinetic properties, the antioxidant, cytotoxic activities in animal cells and antiparasitic activities were evaluated against the different forms of *Leishmania amazonensis* and *Trypanosoma cruzi* *in vitro*. The *in silico* study showed that the evaluated compounds showed good oral availability. In a preliminary *in vitro* study, the compounds showed moderate to low antioxidant activity. Cytotoxicity assays show that the compounds showed moderate to low toxicity. In relation to leishmanicidal activity, the compounds presented IC_{50} values that ranged from 19.86 to 200 μ M for the promastigote form, while for the amastigote forms, IC_{50} ranged from 101 to more than 200 μ M. The compounds showed better results against the forms of *T. cruzi* with IC_{50} ranging from 1.67 to 100 μ M for the trypomastigote form and 1.96 to values greater than 200 μ M for the amastigote form. This study showed that thiazole compounds can be used as future antiparasitic agents.

Key words: antiparasitic, *Leishmania amazonensis*, compounds, *Trypanosoma cruzi*.

INTRODUCTION

Neglected tropical diseases (NTDs) are a group of infectious diseases of protozoan, helminthic, bacterial, viral, and fungal origin, among others, common in tropical and subtropical regions where situations of poverty are common, although there are also records of their presence in non-endemic areas, that is, in developed countries (Elphick-Pooley & Engels 2022, Zhou 2022). These diseases affect more than 1.5 billion people worldwide and are responsible for more than 530000 deaths each year (Ahmed et al. 2022, Naqvi et al. 2022). In this scenario, research on NTDs has increased due to the need to establish monitoring systems and improve existing treatment programs, aiming to control

the impacts of these diseases (Otte & Pica-Ciamarra 2021, Souza et al. 2021, Ahmed et al. 2022, Elphick-Pooley & Engels 2022, Naqvi et al. 2022, Zhou 2022).

Among the different NTDs, there is Leishmaniasis, a disease caused by a parasite of the *Leishmania* genus, which affects about 12 million people a year (Santos et al. 2020). There are still no vaccines available for humans and the drugs used for treatment (pentavalent antimonials, amphotericin B, and miltefosine) can promote parasite resistance in addition to being highly toxic to patients (Santos et al. 2020, Chanda 2021). Like leishmaniasis, Chagas disease is part of the NTD group and affects about 10 million people, it is caused by a parasite called

Trypanosoma cruzi, which is endemic mainly in the Americas and spreads in different European countries, Australia, and Japan (Chanda 2021). The drugs used for the treatment of this disease are benznidazole and nifurtimox, which have limited efficiency in the chronic phase of the disease and have significant side effects, in addition to being contraindicated during pregnancy (Santos et al. 2020, Chanda 2021).

In this context, the search for new treatment therapies for Chagas disease and leishmaniasis has increased, to obtain drugs with low toxicity, which promote fewer side effects and have a shorter treatment time and low cost (Chanda 2021). Therefore, different compounds have been isolated or synthesized to act as new ways of treating NTDs caused by parasites. Among the variety of compounds, there are the thiazoles, pentagonal heteroaromatics, with three carbon atoms, one sulfur, and one nitrogen atom (Petrou et al. 2021). The arrangement of these atoms in the heterocyclic ring can vary in two ways leading to the existence of 1,2-thiazole or 1,3-thiazole. Thiazole is a functional group that occupies a prominent place in medicinal chemistry due to its reactivity and biological activity, is widely found in drugs applied in the fight against diseases in general (Chhabria et al. 2016, Petrou et al. 2021).

Different studies evaluating the leishmanicidal and trypanocidal activity have been carried out, among which we can mention Haroon et al. (2021) evaluating the leishmanicidal and trypanocidal activity of 1, 3-thiazole, and 4-thiazolidinone ester compounds. Oliveira et al. (2020) evaluated different thiazoles against *Leishmania infantum*. Queiroz et al. (2020) evaluated different thiazoles and thiosemicarbazones against forms of *Leishmania infantum*. Martínez-Cerón et al. (2021) evaluate different phenylbenzothiazole compounds against *Trypanosoma cruzi*.

González et al. (2021) performed QSAR studies to assess the potential of different thiazoles also against *Trypanosoma cruzi*. Oliveira-Filho et al. (2017) and Silva et al. (2017) evaluated the action of thiazole compounds against different forms of *Trypanosoma cruzi*. In addition to the potential effect of thiazoles in monotherapy, they can be combined with other drugs to increase the efficiency of the treatment (Scarim et al. 2019, Perdomo et al. 2021).

Therefore, this work aimed to synthesize new thiazole compounds, to evaluate in a preliminary way the biological potential through a pharmacokinetic study (ADME) and to evaluate the activities, cytotoxicity in animal cells and antiparasitic activity against the promastigote and amastigote forms of *Leishmania amazonensis* and against the trypomastigote and amastigote forms of *Trypanosoma cruzi* *in vitro* (Figure 1).

MATERIALS AND METHODS

Reagents

Schneider® culture medium (Merck), 3-(4,5-dimethyltriazol-2-yl)-2,5-diphenyltetrazolium bromide - MTT (Merck, CAS: 298-93-1), RPMI 1640 culture medium (Thermo Fisher Scientific), gentamicin (Novafarma), penicillin (Novafarma), fetal bovine serum (Thermo Fisher Scientific), amphotericin B (Merck, CAS:1397-89-3), miltefosine (Merck, CAS: 58066-85-6), Benzonidazole (Merck, CAS: 22994-85-0), 2,2'-azino-bis(3-ethylbenzothiazoline-6-sulfonic acid) (ABTS; Merck, CAS: 30931-67-0), potassium persulfate (Merck, CAS: 7727-21-1), ascorbic acid (Merck, CAS: 50-81-7), Butylated hydroxytoluene (Merck, CAS:128-37-0), ethanol (Merck, CAS:64-17-5), sodium lauryl sulfate (Merck, CAS:151-21-3), Triton™ X-100 (Merck, CAS:9036-19-5), Giemsa stain (Merck, CAS:51811-82-6), Chlorophenol red-β-D-galactopyranoside (Merck, CAS: 99792-79-7).

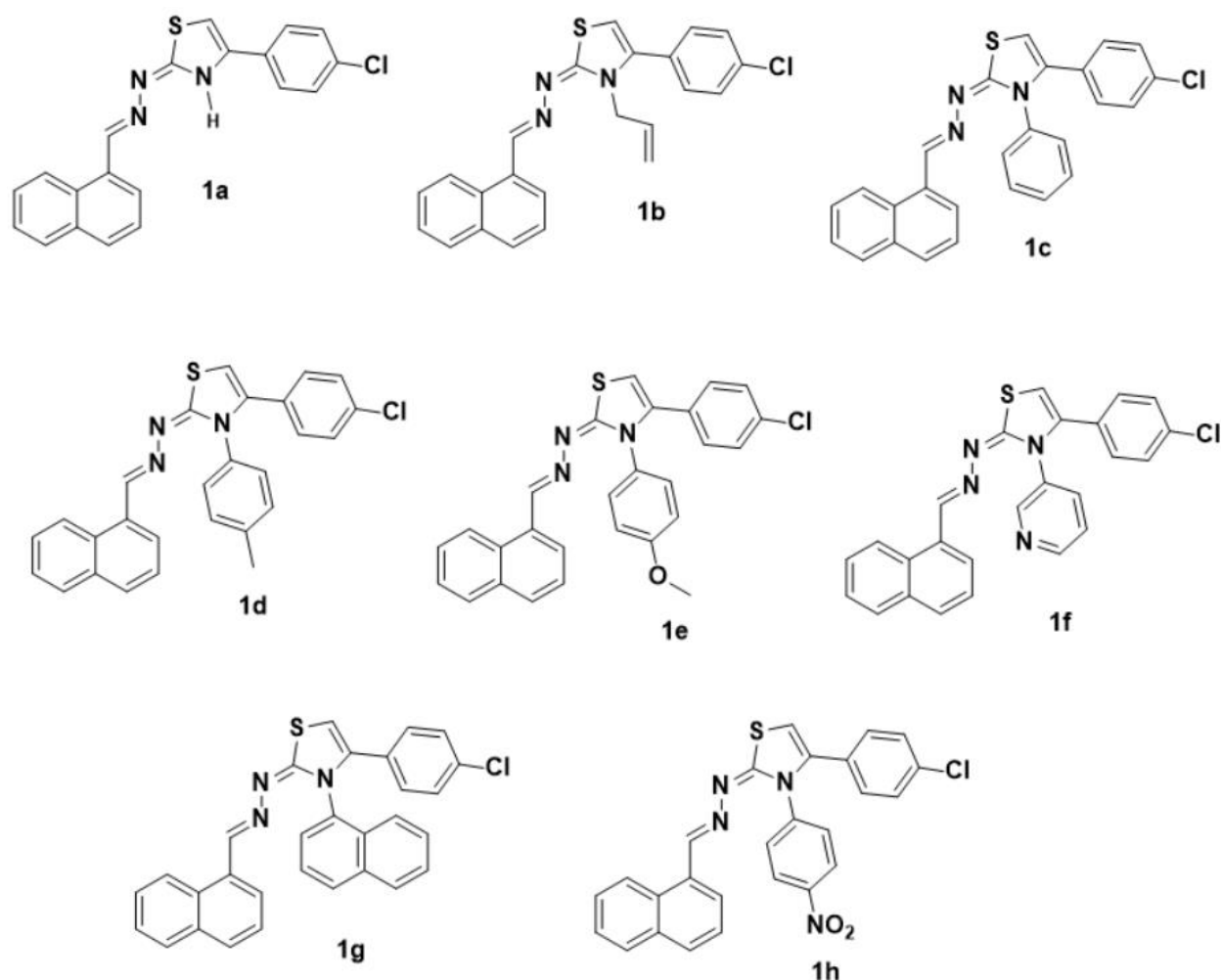


Figure 1. Chemical structures of thiazoles provided by LIQT.

All reagents used were obtained commercially (Fluka and Merck). The development of the reactions was monitored using thin layer chromatography (Merck, silica gel F254 on aluminum foil). The melting points were determined from capillary tubes with the Fisatom device (model 431D 60W, Brazil). The IR spectrum was generated from the Spectrum 400 equipment (Perkin Elmer). NMR spectra were obtained using Bruker AMX-300 MHz devices (300 MHz for ^1H and 75.5 MHz for ^{13}C). Chemical shifts were recorded in δ units and coupling constants (J) were recorded in Hertz (Hz). The multiplicities were displayed as s (singlet), d

(doublet), t (triplet), m (multiplet), dd (double doublet).

Thiazole derivatives

The compounds were synthesized at the Laboratory of Chemistry and Therapeutic Innovation (LQIT) of the Federal University of Pernambuco (UFPE), Recife, Pernambuco, Brazil. The thiazole derivatives (1a-h) were obtained in three steps. First, thiosemicarbazides were synthesized from hydrazine hydrate and substituted isothiocyanate in dichloromethane. Then, thiosemicarbazones were obtained according to the methodology proposed by Oliveira et al. (2015) and Jacob et al. (2021) with

few modifications, from thiosemicarbazides with 1-naphthyl-carboxaldehyde. Finally, thiazoles (1a -h) were obtained from thiosemicarbazones, which were subjected to Hantzsch condensation with 2-bromo-4'-chloroacetophenone according to the methodology described by Oliveira-Filho et al. (2017) and Alves et al. (2021).

The synthesis diagram (Figure S1) and spectra for each of the compounds are shown in the supplementary material.

Compound (1a): 4-(4-chlorophenyl)-2-[2-(naphthalen-1-ylmethylene)-hydrazinyl]-1,3-thiazole

Orange powder; MP 176-178 °C; Yield: 62.5%; Rf: 0.70 (*n*-hexane/ethyl acetate 8:2). NMR ¹H (400 MHz, DMSO-d₆) δ ppm: 7.38 (s, 1H, CH thiazole), 7.45 (d, *J* = 8.0 Hz, 2H, CH *p*-chlorophenyl), 7.54-7.58 (m, 2H, CH naphthyl), 7.63-7.66 (m, 1H, CH naphthyl), 7.84 (d, 1H, CH naphthyl), 7.87 (d, *J* = 8.0 Hz, 2H, CH *p*-chlorophenyl), 7.94-7.98 (m, 2H, CH naphthyl), 8.68 (s, 1H, CH), 8.75 (d, *J* = 8.0 Hz, 1H, CH naphthyl), 12.27 (s, 1H, NH). NMR ¹³C (100 MHz, DMSO-d₆) δ ppm: 104.9 (CH thiazole), 124.4, 126.0, 126.6, 127.4, 127.6, 127.7, 129.0, 129.2, 129.9, 130.23, 130.26, 132.4, 133.9, 134.0, 141.9, 149.9, 168.8. FT-IR (ATR, cm⁻¹): 3173 (NH), 1568 (C=N). HRMS *m/z* [M + H]⁺ calculated for C₂₀H₁₄ClN₃S: 363.059.

Compound (1b): 3-allyl-4-(4-chlorophenyl)-2-((naphthalen-1-ylmethylene)-hydrazinylidene)-2,3-dihydrothiazole

Yellow powder; MP 114-115 °C; Yield: 40.9%; Rf: 0.85 (*n*-hexane/ethyl acetate 8:2). NMR ¹H (300 MHz, DMSO-d₆) δ ppm: 4.45 (d, *J* = 3.0 Hz, 2H, CH₂ allyl), 4.92 (d, *J* = 18.0 Hz, 1H, =CH₂ allyl), 5.12 (d, *J* = 12.0 Hz, 1H, =CH₂ allyl), 5.79-5.91 (m, 1H, =CH allyl), 6.50 (s, 1H, CH thiazole), 7.48-7.66 (m, 7H, CH *p*-chlorophenyl and naphthyl), 7.92 (d, *J* = 6.0 Hz, 1H, CH naphthyl), 7.95 (d, *J* = 9.0 Hz, 1H, CH naphthyl), 7.99 (d, *J* = 9.0 Hz, 1H, CH naphthyl), 8.89 (s, 1H, CH), 9.07 (d, *J* = 9.0 Hz, 1H, CH naphthyl).

NMR ¹³C (75 MHz, DMSO-d₆) δ ppm: 47.4, 101.1 (CH thiazole), 116.4, 125.1, 125.5, 126.1, 127.1, 128.4, 128.6, 128.7, 129.3, 129.7, 130.1, 130.4, 130.5, 132.6, 133.6, 134.0, 139.1, 151.2, 169.3. FT-IR (ATR, cm⁻¹): 1571 (C=N). HRMS *m/z* [M + H]⁺ calculated for C₂₃H₁₈ClN₃S: 403.091.

Compound (1c): 4-(4-chlorophenyl)-2-((naphthalen-1-ylmethylene)-hidrazineylidene)-3-phenyl-2,3-dihydrothiazole.

Yellow powder; MP 208-210 °C; Yield: 67.4%; Rf: 0.70 (*n*-hexane/ethyl acetate 8:2). NMR ¹H (300 MHz, DMSO-d₆) δ ppm: 6.75 (s, 1H, CH thiazole), 7.20 (d, *J* = 9.0 Hz, 2H, CH *p*-chlorophenyl), 7.30-7.42 (m, 6H, CH *p*-chlorophenyl and phenyl), 7.56-7.65 (m, 3H, CH naphthyl), 7.89 (d, *J* = 9.0 Hz, 1H, CH naphthyl), 7.96 (d, *J* = 6.0 Hz, 1H, CH naphthyl), 7.98 (d, *J* = 9.0 Hz, 1H, CH naphthyl), 8.75 (s, 1H, CH), 9.05 (d, *J* = 9.0 Hz, 1H, CH naphthyl). NMR ¹³C (75 MHz, DMSO-d₆) δ ppm: 102.4 (CH thiazole), 125.2, 125.4, 126.1, 127.1, 128.1, 128.2, 128.6, 128.71, 128.76, 129.0, 129.5, 129.9, 130.06, 130.09, 130.3, 133.1, 133.5, 137.3, 138.6, 152.2, 170.1. FT-IR (ATR, cm⁻¹): 1587 (C=N). HRMS *m/z* [M + H]⁺ calculated for C₂₆H₁₈ClN₃S: 439.091.

Compound (1d): 4-(4-chlorophenyl)-2-((naphthalen-1-ylmethylene)-hydrazono)-3-(*p*-tolylphenyl)-2,3-dihydrothiazole.

Yellow powder; MP 223-225 °C; Yield: 78.0%; Rf: 0.88 (*n*-hexane/ethyl acetate 8:2). NMR ¹H (300 MHz, DMSO-d₆) δ ppm: 2.31 (s, 3H, CH₃), 6.72 (s, 1H, CH thiazole), 7.21 (s, 6H, CH *p*-chlorophenyl and *p*-methylphenyl), 7.33 (d, *J* = 6.0 Hz, 2H, CH *p*-chlorophenyl), 7.57-7.62 (m, 3H, CH naphthyl), 7.88 (d, *J* = 6.0 Hz, 1H, CH naphthyl), 7.96 (d, *J* = 6.0 Hz, 1H, CH naphthyl), 7.98 (d, *J* = 6.0 Hz, 1H, CH naphthyl), 8.73 (s, 1H, CH), 9.04 (d, *J* = 9.0 Hz, 1H, CH naphthyl). NMR ¹³C (75 MHz, DMSO-d₆) δ ppm: 20.6, 102.2 (CH thiazole), 125.2, 125.4, 126.1, 127.1, 128.3, 128.4, 128.70, 128.76, 129.3, 129.5, 129.9, 130.1, 130.2, 130.3, 133.1, 133.5, 134.7, 137.5, 138.7, 152.0,

170.3. FT-IR (ATR, cm^{-1}): 1585 (C=N). HRMS m/z [$M + H$]⁺ calculated for $\text{C}_{27}\text{H}_{20}\text{ClN}_3\text{S}$: 453.106.

Compound (1e): 4-(4-chlorophenyl)-3-(4-methoxyphenyl)-2-((naphthalen-1-ylmethylene)-hydrazineylidene)-2,3-dihydrothiazole.

Yellow powder; MP 227-229 °C; Yield: 55.4%; Rf: 0.73 (*n*-hexane/ethyl acetate 8:2). NMR ^1H (300 MHz, DMSO-d_6) δ ppm: 3.77 (s, 3H, OCH_3), 6.71 (s, 1H, CH thiazole), 6.95 (d, $J = 9.0$ Hz, 2H, CH *p*-methoxyphenyl), 7.23 (d, $J = 9.0$ Hz, 2H, CH *p*-chlorophenyl), 7.26 (d, $J = 9.0$ Hz, 2H, CH *p*-methoxyphenyl), 7.34 (d, $J = 9.0$ Hz, 2H, CH *p*-chlorophenyl), 7.54-7.65 (m, 3H, CH naphthyl), 7.87 (d, $J = 9.0$ Hz, 1H, CH naphthyl), 7.96 (d, $J = 6.0$ Hz, 1H, CH naphthyl), 7.98 (d, $J = 9.0$ Hz, 1H, CH naphthyl), 8.73 (s, 1H, CH), 9.04 (d, $J = 9.0$ Hz, 1H, CH naphthyl). NMR ^{13}C (75 MHz, DMSO-d_6) δ ppm: 55.3, 101.9 (CH thiazole), 114.2, 124.9, 125.5, 126.1, 126.4, 127.1, 128.3, 128.6, 129.0, 129.6, 130.2, 130.3, 131.6, 133.5, 133.8, 139.1, 151.9, 158.7, 170.5. FT-IR (ATR, cm^{-1}): 1583 (C=N). HRMS m/z [$M + H$]⁺ calculated for $\text{C}_{27}\text{H}_{20}\text{ClN}_3\text{OS}$: 469.101.

Compound (1f): (E)-4-(4-chlorophenyl)-2-((naphthalen-1-ylmethylene)hydrazono)-3-(pyridin-3-yl)-2,3-dihydrothiazole.

Yellow powder; MP 248-250; Yield: 51.7%; Rf: 0.27 (hexane/ethyl acetate 8:2). NMR ^1H (300 MHz, DMSO-d_6) δ ppm: 6.80 (s, 1H, CH thiazole), 7.25 (d, $J = 9.0$ Hz, 2H, CH *p*-chlorophenyl), 7.37 (d, $J = 9.0$ Hz, 2H, CH *p*-chlorophenyl), 7.46-7.50 (m, 1H, CH pyridyl), 7.55-7.65 (m, 3H, CH naphthyl), 7.85 (d, $J = 9.0$ Hz, 1H, CH naphthyl), 7.90 (d, $J = 6.0$ Hz, 1H, CH naphthyl), 7.98 (d, $J = 9.0$ Hz, 1H, CH naphthyl), 8.00 (d, $J = 6.0$ Hz, 1H, CH naphthyl), 8.53 (d, $J = 3.0$ Hz, 1H, CH pyridyl), 8.54 (d, $J = 9.0$ Hz, 1H, CH pyridyl), 8.77 (s, 1H, CH), 9.05 (d, $J = 6.0$ Hz, 1H, CH naphthyl). NMR ^{13}C (75 MHz, DMSO-d_6) δ ppm: 102.8 (CH thiazole), 109.5, 123.5, 125.1, 125.5, 126.1, 127.2, 128.5, 128.6, 129.0, 129.5, 129.9, 130.11, 130.4,

133.4, 133.5, 134.1, 136.4, 140.1, 148.7, 149.3, 152.9, 168.7. FT-IR (ATR, cm^{-1}): 1583 (C=N). HRMS m/z [$M + H$]⁺ calculated for $\text{C}_{25}\text{H}_{17}\text{ClN}_4\text{S}$: 440.086; found: 440.103.

Compound (1g): 4-(4-chlorophenyl)-3-(naphthalen-1-yl)-2-(naphthalen-1-ylmethylene)hydrazono)-2,3-dihydrothiazole

Yellow powder; MP 280-282 °C; Yield: 63.7%; Rf: 0.69 (hexane/ethyl acetate 8:2). NMR ^1H (400 MHz, DMSO-d_6) δ ppm: 7.00 (s, 1H, CH thiazole), 7.16 (m, 4H, CH *p*-chlorophenyl), 7.51-7.64 (m, 7H, CH naphthyl), 7.77 (d, $J = 8.0$ Hz, 1H, CH naphthyl), 7.82 (d, $J = 8.0$ Hz, 1H, CH naphthyl), 7.94-7.97 (m, 2H, CH naphthyl), 7.99-8.03 (m, 2H, CH naphthyl), 8.62 (s, 1H, CH), 8.91 (d, $J = 8.0$ Hz, 1H, CH naphthyl). NMR ^{13}C (100 MHz, DMSO-d_6) δ ppm: 104.0 (CH thiazole), 122.5, 125.3, 125.9, 126.2, 126.6, 127.2, 127.7, 128.3, 128.6, 128.9, 129.0, 129.1, 129.2, 129.3, 130.20, 130.23, 130.35, 130.39, 130.5, 130.8, 133.3, 134.01, 134.09, 134.3, 140.1, 152.8, 170.8. FT-IR (ATR, cm^{-1}): 1593 (C=N). HRMS m/z [$M + H$]⁺ calculated for $\text{C}_{30}\text{H}_{20}\text{ClN}_3\text{S}$: 489.106; found: 489.125.

Compound (1h): (E)-4-(4-chlorophenyl)-2-((naphthalen-1-ylmethylene)hydrazineylidene)-3-(4-nitrophenyl)-2,3-dihydrothiazole

Yellow powder; MP 201-203; Yield: 78.8%; Rf: 0.72 (hexane/ethyl acetate 8:2). NMR ^1H (300 MHz, DMSO-d_6) δ ppm: 6.83 (s, 1H, CH thiazole), 7.23 (d, $J = 9.0$ Hz, 2H, CH *p*-chlorophenyl), 7.35 (d, $J = 9.0$ Hz, 2H, CH *p*-chlorophenyl), 7.54-7.64 (m, 3H, CH naphthyl), 7.65 (d, $J = 9.0$ Hz, 2H, CH *p*-nitrophenyl), 7.90 (d, $J = 9.0$ Hz, 1H, CH naphthyl), 7.97-8.01 (m, 2H, CH naphthyl), 8.26 (d, $J = 9.0$ Hz, 2H, CH *p*-nitrophenyl), 8.78 (s, 1H, CH), 9.04 (d, $J = 9.0$ Hz, 1H, CH naphthyl). NMR ^{13}C (75 MHz, DMSO-d_6) δ ppm: 103.8 (CH thiazole), 124.1, 125.1, 125.5, 126.1, 127.2, 128.5, 128.7, 129.0, 129.1, 129.9, 130.03, 130.06, 130.1, 130.3, 133.4, 133.5, 137.7, 142.8, 146.1, 153.4, 169.3. FT-IR (ATR, cm^{-1}): 1585 (C=N). HRMS m/z [$M + H$]⁺ calculated for $\text{C}_{26}\text{H}_{17}\text{ClN}_4\text{O}_2\text{S}$: 484.076.

Preparation of solutions of compounds

All compounds evaluated in this study were solubilized in dimethylsulfoxide (DMSO), according to the methodology proposed by Jacob et al. (2021) with few modifications to obtain a concentration of 800 μM . Then, they were diluted in different concentrations. Dilutions were performed in phosphate-buffered saline to obtain a final concentration of 1% DMSO.

Prediction of Pharmacokinetic Properties

The *in silico* study of the compounds was carried out in order to predict pharmacokinetic and physicochemical properties (Norinder & Bergström 2006). Knowledge of properties such as absorption, distribution, metabolism and excretion (ADME) are indispensable in the process of developing new drug candidate molecules and help predict the oral bioavailability of new drug candidates (Pires et al. 2015). For this, we use the software available online SwissADME (<http://www.swissadme.ch>) and pkCSM (<http://biosig.unimelb.edu.au/pkcsm/prediction>).

The parameters evaluated were: molecular weight, number of hydrogen bond acceptors, number of hydrogen bond donors, log P, total polar surface area, LogS, permeability in Caco-2, intestinal absorption, volume of distribution, unbound and total fraction clearance.

In vitro antioxidant activity

ABTS radical capture method

Antioxidant activity by the ABTS [2,2'-azinobis-(3-ethylbenzothiazoline-6-sulfonic acid)] method was performed according to the methodology described by Salar et al. (2017) with modifications. The ABTS radical was formed by reacting 5 mL of the ABTS solution 7mM with 88 μL of 140mM potassium persulfate solution, incubated at 25°C and in the absence of light, for

16 hours. Once formed, the radical was diluted with ethanol P.A. until obtaining the absorbance value of 0.70 ± 0.020 at 734 nm.

Compounds in a volume of 0.5 mL at different concentrations (6 – 5000 μM) were added to 3.5 mL of the reagent, then the system was kept in the dark for 30 minutes. Then the assays were analyzed in a spectrophotometer at 734 nm. The equipment blank was ethanol. The standards used were ascorbic acids and butylated hydroxytoluene (BHT) under the same conditions as the compounds. The percentage of radical capture was determined through Equation 1.

$$\text{ABTS (\%)} = \left(\frac{\text{ABS control} - \text{ABS sample}}{\text{ABS control}} \right) * 100 \quad (1)$$

Where: ABS control is the absorbance of the control and ABS Sample is the absorbance of the sample containing the compounds after testing.

The IC_{50} (concentration capable of capturing 50% of the radicals) was determined by non-linear regression analysis of data obtained by SPSS 8.0 software for Windows. The results were expressed in concentrations of μM .

DPPH radical capture method

The assay to determine the antioxidant activity by the 1,1-diphenyl-2-picrylhydrazine (DPPH) method was performed according to the methodology described by Andreani et al. (2013) with modifications. The technique consists of the reaction of the free radical DPPH 0.03mM with the compounds in ethanolic solution, for 30 minutes. Compounds in a volume of 0.5 mL at different concentrations (6 – 5000 μM) were added to 3.5 mL of the reagent, then the system was kept in the dark for 30 minutes. Then the assays were analyzed in a spectrophotometer at 517 nm. The equipment blank was ethanol. The standards used were ascorbic acids and butylated hydroxytoluene (BHT) under the same

conditions as the compounds. The percentage of radical capture was determined through Equation 1.

The IC_{50} (concentration capable of capturing 50% of the radicals) was determined by non-linear regression analysis of data obtained by SPSS 8.0 software for Windows. The results were expressed in concentrations of μM .

Cytotoxicity assays in animal cells

In vitro hemolytic activity

The assay was performed according to Queiroz et al. (2020) and Ansari et al. (2020) with some modifications. Hemolytic activity was performed in 96-well microplates. Erythrocytes were isolated by centrifugation (1500 rpm, 10 min at 4°C). Subsequently, they were washed three times with phosphate-buffered saline (PBS; pH 7.4). Then, each tube received 1.1 mL of erythrocyte suspension (1%) and 0.4 mL of various concentrations of compounds (0 to 200 μM). Distilled water (negative) and Triton X100 (0.0025%, positive) were used as controls. After 60 minutes of incubation, the cells were centrifuged and the absorbance of the supernatant was recorded at 540 nm. The hemolytic activity results were expressed by the following Equation 4.

$$\text{Hemolysis (\%)} = \left[\frac{\text{ABS sample} - \text{ABS blank}}{\text{ABS Triton X} - \text{ABS blank}} \right] * 100 \quad (1)$$

Where: ABS sample: Sample absorbance, ABS blank: negative control absorbance, ABS Triton X: positive control absorbance.

The effective concentration that promotes 50% of hemolysis (IC_{50}) was determined. Three independent experiments were performed in triplicate. The study was approved by the Ethics Committee on the Use of Animals of the Aggeu Magalhães Institute/Oswaldo Cruz Foundation, protocol number 164/2020.

Cytotoxicity assays in RAW.264.7 macrophage cells, V79 fibroblasts and hepatoma (HepG2)

Assays were performed according to Palanimuthu & Samuelson (2013), Ruiz et al. (2010), and Gouveia et al. (2022) with few modifications. For this purpose, macrophage strains RAW.264.7, V79 fibroblasts, and hepatoma (HepG2) were used and maintained under culture conditions at the Immunogenetics Laboratory of Aggeu Magalhães Institute, Oswaldo Cruz Foundation, Recife, PE, Brazil. Cells were grown in cell culture bottles (75 cm^3 , corresponding to 250 mL), and maintained in RPMI 1640 medium with phenol red. For supplementation of the culture medium, 10% fetal bovine serum was used, the antibiotics penicillin, 100 U/mL, and streptomycin, 100 $\mu\text{g}/\text{mL}$, and the buffer solution HEPES (4-(2-hydroxyethyl)-1-piperazineethanesulfonic acid).

Assays were performed in 96-well culture plates and monitored under a microscope. 100 μL of RPMI-1640 medium, supplemented with fetal bovine serum, containing 10^4 cells in each well was added to the plates. The plates were incubated in a 5% CO_2 oven at 37 °C for 24 hours. After this incubation period, compounds were added to the cells at concentrations from 0 to 200 μM in triplicate on each plate. The plates were incubated again in a CO_2 oven for 72 hours.

After this period, 20 μL of 3-(4,5-dimethyltriazol-2-yl)-2,5-diphenyltetrazolium bromide (MTT) solution at 0.5 mg/mL was added to each well. The plates were incubated for another 3 hours for the MTT to react with the cells and form the insoluble crystals of Formazan. After 3 hours, 100 μL of supernatant were removed from each well and discarded, and later, 130 μL of sodium lauryl sulfate solution was added to dissolve the formed crystals. After 24 hours it was possible to read the absorbance in a plate spectrophotometer at

570 nm. With the absorbance values obtained by reading, it was possible to obtain the percentage of cell viability (amount of live cells) resulting from the treatment with each tested compound in its proper concentrations. In addition to the compounds studied here, tests were also carried out for comparison purposes using the standard drug amphotericin B, miltefosine, and benznidazole (dissolved under the same conditions as the compounds). The experiments were performed in triplicate and biological replication and cell viability and inhibition were calculated using Equations 2 and 3.

$$\text{Cell viability (\%)} = \left(\frac{\text{VC}}{\text{TC}} \right) * 100\% \quad (2)$$

$$\text{Inhibition of cel Growth(\%)} = 100 - \text{cell viability} \quad (3)$$

Where: VC is the number of cells at different concentrations, TC is the concentration of cells in the control which represents 100% viability.

The effective concentration that promotes 50% of cell viability (CC_{50}) was determined by non-linear regression analysis of data obtained by SPSS 8.0 software for Windows.

Evaluation of *in vitro* leishmanicidal activity

Cultivation and maintenance of parasites

The experiments were carried out according to Gouveia et al. (2022) with few modifications. The promastigote forms of *Leishmania amazonensis* were maintained in supplemented Schneider medium (20% fetal bovine serum and 1% streptomycin penicillin solution), pH 7.2 at 26 °C. Parasites in the exponential phase of growth were used in all experiments with re-raising every three days. Then, they were subjected to three cycles of washing with cold sterile saline, with centrifugation at 3000 rpm, for 15 minutes at 4 °C and adjusted with Schneider medium to

the desired concentrations in each experiment. The viability of the parasites was analyzed by light microscopy. The amastigote forms were obtained after incubation and internalization of the promastigote forms in macrophage culture.

Growth kinetics of promastigote forms

The parasites in the promastigote form were maintained at 26 °C in supplemented Schneider medium (20% fetal bovine serum and 1% penicillin-streptomycin solution), pH 7.2. The growth curve was performed according to Gouveia et al. (2022) and Silva et al. (2020) with modifications. To carry out the experiments, an initial concentration of 1×10^6 cells/well of parasites was used, grown in 96-well plates in an atmosphere of 5% CO_2 at 37 °C at times ranging from 0 to 120 hours. Culture growth was monitored by counting in a Neubauer chamber. The experiments were carried out in triplicate.

Cytotoxicity of promastigote forms *in vitro*

The cytotoxicity experiments in promastigote forms were carried out according to a methodology adapted from Gouveia et al. (2022) and Silva et al. (2020) with few modifications. The experiments were performed on 96-well plates. Promastigote forms were grown in Schneider's medium supplemented for 72 hours and counted in a Neubauer chamber at a final concentration of 1×10^6 cells/well. Then these forms were incubated in the presence of different concentrations (0 to 200 μM) of the compounds for 72 hours. The positive control used was the drugs Amphotericin B and Miltefosine (under the same experimental conditions as the compounds) and the negative control was the culture medium and only cells, respectively. Viability was evaluated by counting in a Neubauer chamber. Through graphs of inhibition against concentrations, it was possible to determine the IC_{50} (concentration of

inhibition of growth by 50%) through non-linear regression analysis by SPSS 8.0 software for Windows. Assays were performed in biological and technical triplicate.

Cytotoxicity of amastigote forms *in vitro*

The tests were performed according to Gouveia et al. (2022) and Silva et al. (2020) with modifications. Initially, RAW.264.7 macrophage cells at a concentration of 1.0×10^5 cells/well were grown in 96-well microplates and incubated at 37°C and 5% CO₂ for 24 hours. After growth, macrophages were infected with the promastigote forms grown in 72 hours, in a ratio of 10:1 parasite macrophage for 24 hours. After this period, the parasites that did not infect the macrophages were removed by 10 washes with RPMI 1640 medium. Then, the infected cells were exposed to different concentrations of the compounds (0 to 200 µM). as a positive control, the drugs Amphotericin B and Miltefosine were used under the same conditions as the compounds. Assays were incubated for 72 hours at 37 °C and 5% CO₂. After 72 hours of treatment, the plates were washed with PBS, fixed with methanol and stained with Giemsa.

The percentage of infected macrophages was determined by counting 100 cells in triplicate. IC₅₀ was determined by non-linear regression analysis of data obtained by SPSS 8.0 software for Windows. Assays were performed in biological and technical triplicate.

Evaluation of cytotoxic activity against the forms of *Trypanosoma cruzi* *in vitro*

Culture of Trypomastigotes

After reaching 100% confluence in culture, RAW.264.7 macrophage cells were infected with 1×10^7 trypomastigotes (Y strain) and cultured in RPMI medium + 5% fetal bovine serum. After 7 days, cells began to release new trypomastigotes

and new RAW.264.7 macrophage cell culture bottles were infected.

Evaluation of the cytotoxicity of the compounds against trypomastigote forms

The tests were carried out according to Oliveira-Cardoso et al. (2014) with modifications, the trypomastigote forms (Y strain) were obtained from the *in vitro* infection (1×10^7 parasites) of the macrophage cell line RAW.264.7, after they reached confluence in culture. To determine the antiproliferative effect for trypomastigote forms of strain Y (1×10^6 parasites/well), maintained in RPMI medium + 1 % antibiotic + 5 % fetal bovine serum, were seeded in 96-well plates at 37 °C, together with different concentrations. of compounds (0 to 200 µM) for 24 hours in a 5% CO₂ atmosphere. Each compound was tested in triplicate. Untreated wells were obtained as a negative control of the reaction and the reference drug used as a positive control was Benznidazole. The parasite viability was determined by direct counting in a Neubauer chamber and, from these values, the IC₅₀ was obtained through a simple linear regression using the Prisma 5.0 Graphpad software.

Evaluation of the cytotoxicity of the compounds against amastigote forms

The tests were carried out according to Oliveira-Cardoso et al. (2014) with modifications. The trypomastigote forms were obtained from the *in vitro* infection of the macrophage strain RAW.264.7. To obtain amastigotes, RAW.264.7 macrophages were seeded in 96-well plates, and incubated for 24 hours at 37°C and an atmosphere with 5% CO₂. Parasites were added at the rate of 10 trypomastigotes/cell. After 24 hours, the non-internalized parasites were removed, and the plates were incubated for 48 hours. The compounds were added at different concentrations (0 to 200 µM), and the plates

were incubated for 96 hours. Wells containing only culture medium and cells were the negative control and wells containing Benzimidazole (diluted under the same experimental conditions as the compounds) the positive control. At the end of the incubation, Chlorophenol red- β -D-galactopyranoside (CPRG), 500 μ M, 0.5% Nonidet P-40, in PBS, was added and incubated for 18 hours at 37°C. The absorbance was read at 570 nm on the Thermo Scientific Multiskan FC spectrophotometer. IC₅₀ values were calculated by regression analysis using GraphPad Prism software. Each assay was performed in triplicate.

Determination of the selectivity index (SI) and specificity index (SPI) of the compounds for the different forms of *Leishmania amazonensis* and *Trypanosoma cruzi*

The SI demonstrates the relationship of compound toxicity between mammalian cells and parasitic forms. It was obtained by the ratio between the value of the cytotoxic concentration (CC₅₀) of the compound in mammalian cells, and the inhibitory concentration (IC₅₀) in promastigote/trypomastigote and amastigotes (Silva et al. 2020, Gouveia et al. 2022). The SPI establishes the specificity of the compound between the two forms of the parasite, promastigote and amastigote. It was calculated by the ratio between the compound IC₅₀ for promastigote/trypomastigote forms and the amastigote IC₅₀ (Gouveia et al. 2022).

Statistical analysis

The results obtained were expressed as mean \pm standard deviation and submitted to analysis of variance (ANOVA) and the means were submitted to Tukey's test ($p \leq 0.05$) using the GraphPad Prism 5.0 software (test version).

RESULTS AND DISCUSSION

***In silico* pharmacokinetic properties**

Theoretical *in silico* pharmacokinetics is an approach currently widely used in the initial study of ADME properties (absorption, distribution, metabolism and excretion) that aims to reduce unnecessary expenditure in biological assays of compounds (Fowler et al. 2022). A good pharmacokinetic profile increases the likelihood that a promising drug candidate will offer a successful therapy (Liu & Shah 2022). Two common ways to assess the potential oral bioavailability of a compound are through the rules proposed by Lipinski (hydrogen donors ≤ 5 , hydrogen bond acceptors ≤ 10 , molecular weight < 500 g/mol, logP < 5 (or MLogP < 4.15) and Veber (rotational bonds ≤ 10 and polar surface area (TPSA) ≤ 140 Å²) are described in Table I (Domínguez-Villa et al. 2021, Bilen et al. 2022, Tabti et al. 2022).

The results show that compounds 1a, 1b and 1f obeyed Lipinski and Veber's rules, but compounds 1c, 1d, 1e, 1g and 1h showed high values of lipophilicity, violating Lipinski's rule in this parameter. Therefore, the compound may violate only one of these parameters to be a drug candidate. Therefore, these rules allow a good prediction of the oral bioavailability profile for new molecules. Other important properties were also evaluated, such as aqueous solubility, expressed numerically by LogS (Tabti et al. 2022). This parameter significantly affects the absorption and distribution characteristics. In general, a compound with low solubility is not well absorbed by the body (Domínguez-Villa et al. 2021, Bilen et al. 2022). Aqueous solubility is the inverse of lipophilicity, the ligands used in this study are classified in the following order: insoluble $< -10 < \text{slightly soluble} < -6 < \text{moderately soluble} < -4 < \text{soluble} < -2 < \text{very soluble} < 0 < \text{highly soluble}$ (Pires et al. 2015). All compounds

Table I. *In silico* pharmacokinetic properties: adsorption, distribution, metabolism and excretion for the compounds under study.

Parameters	1a	1b	1c	1d	1e	1f	1g	1h
Mw (g/mol) ^a	363.86	403.93	439.96	453.99	469.99	440.95	490.02	484.96
HBA ^b	2	2	2	2	3	3	2	4
HBD ^c	1	0	0	0	0	0	0	0
LogP ^d	4.18	4.76	5.50	5.70	5.12	4.45	6.12	5.31
TPSA (Å ²) ^e	68.75	57.89	57.89	57.89	67.12	70.78	57.89	103.71
LogS ^f	-6.90	-7.52	-8.48	-8.85	-8.64	-7.64	-9.77	-9.26
Caco-2 perm. ^g	1.05	1.11	1.09	1.08	1.08	1.13	1.05	0.24
Int. abs (%) ^h	91.98	95.1	95.91	95.86	96.81	98.17	97.38	92.71
VDSS(LogL/kg) ⁱ	0.24	0.60	0.17	0.231	0.20	0.71	-0.26	0.006
Fract. Unb ^j	0.01	0.11	0.24	0.25	0.26	0.24	0.30	0.23
Total clearance (log mL/min/kg) ^k	0.20	0.25	0.12	0.07	0.16	0.26	0.28	0.15

^aSwissADME Molecular Weight; ^bSwissADME Number H-bonds acceptors; ^cSwissADME Number H-bonds donors; ^dSwissADME Moriguchi log of octanol-water partition coefficient; ^eSwissADME Ali log of aqueous solubility; ^fSwissADME calculation of Topological Polar Surface Area (TPSA); ^gpkCSM prediction of Caco-2 cell permeability as estimation of absorption at human intestinal mucosa; ^hpkCSM prediction of the proportion of compound absorption through the human small intestine; ⁱpkCSM prediction of the log of steady state volume of distribution (VDss); ^jpkCSM prediction of compound fraction unbound in plasma (not bound to serum proteins); ^kpkCSM prediction of the log of total drug clearance.

have low solubility and are classified as slightly soluble.

Through the pkCMS platform, some important pharmacokinetic properties were predicted for the ligands under study, such as the permeability value of Caco-2 cells, which provides an estimate for the absorption of the compound in the human intestinal mucosa. Thus, the results allow classifying the compounds as poorly absorbed ($< 1 \times 10^{-6}$ cm/s), moderately absorbed (1 between 10×10^{-6} cm/s) and well absorbed ($> 10 \times 10^{-6}$ cm/s). Compound 1h is classified as poorly absorbed and the other compounds are classified as moderately absorbed. The compounds showed a percentage of absorption through the intestine of greater than 90% (Pires et al. 2015).

The volume of distribution (VDss) is the parameter that describes the extent of drug

distribution in tissues and plasma. VDss values (log VDss) > 0.45 indicate that the drug will be distributed into the tissue. Log VDss values < -0.15 indicate that the drug will be distributed in plasma (Pires et al. 2015, Tabti et al. 2022). The results show that the compounds have a higher affinity to be distributed in tissues, since all VDss values were > -0.15 with the exception of compound 1g, which presented a VDss value of -0.26 with greater distribution in plasma.

The compounds have a low fraction bound to serum protein. In addition, they present a low clearance rate between 0.07 and 0.28. Therefore, the evaluated compounds showed good ADME results indicating potential oral bioavailability.

***In vitro* antioxidant activity**

The antioxidant activity was evaluated through the ABTS and DPPH radical scavenging assay

of compounds 1a – 1h. Activity results were presented at IC_{50} (concentration capable of capturing radicals by 50%). For the ABTS assays, the values ranged from 322.4 to 2091.1 μ M, showing low antioxidant activity when compared to the standard's ascorbic acid (76.9 μ M) and butylated hydroxytoluene (28.6 μ M). Only compounds 1a (322.4 \pm 0.1 μ M), 1d (1836.2 \pm 1.9 μ M), 1e (2091.1 \pm 1.5 μ M) and 1f (1823.4 \pm 1.0 μ M) showed IC_{50} . ABTS results for each of the compounds are shown in the supplementary material (Table S1). In relation to the DPPH assays none of the compounds presented IC_{50} values, in the highest concentration the percentage of capture varied from 23.7 to 35%. This difference in results may be related to the versatility of the ABTS assay. This is capable of evaluating compounds of a hydrophobic nature (the compounds were more hydrophobic as shown in the *in silico* study) and hydrophilic, unlike the DPPH test, which presents good results for compounds that have a mostly hydrophilic character (Shalaby & Shanab 2013, Moharram & Youssef 2014).

In the literature, different studies report that thiazole compounds are molecules

capable of promoting antioxidant activity both *in vitro* and *in vivo*, and this potential activity is directly related to the chemical structure of these compounds (Salar et al. 2017, Khamees et al. 2019, Dincel et al. 2020). However, the 2-chlorophenylthiazoles compounds did not show antioxidant activity.

Cytotoxicity assays in animal cells: erythrocytes, macrophages RAW.264.7, fibroblasts (V79) and hepatoma (HepG2)

Cytotoxicity in erythrocytes is one of the experimental models of *in vitro* toxicity that stands out as a screening method (Amin & Dannenfelser 2006). This is because it is an easy, fast and efficient method to evaluate the effects of compounds on the cell membrane of erythrocytes (Amin & Dannenfelser 2006, Marques-Garcia 2020). Figure 2 presents the results of hemolytic activity promoted by the compounds at different concentrations. The negative control consisted only of erythrocytes (0% hemolysis) and the positive one contained Triton-X (100% hemolysis).

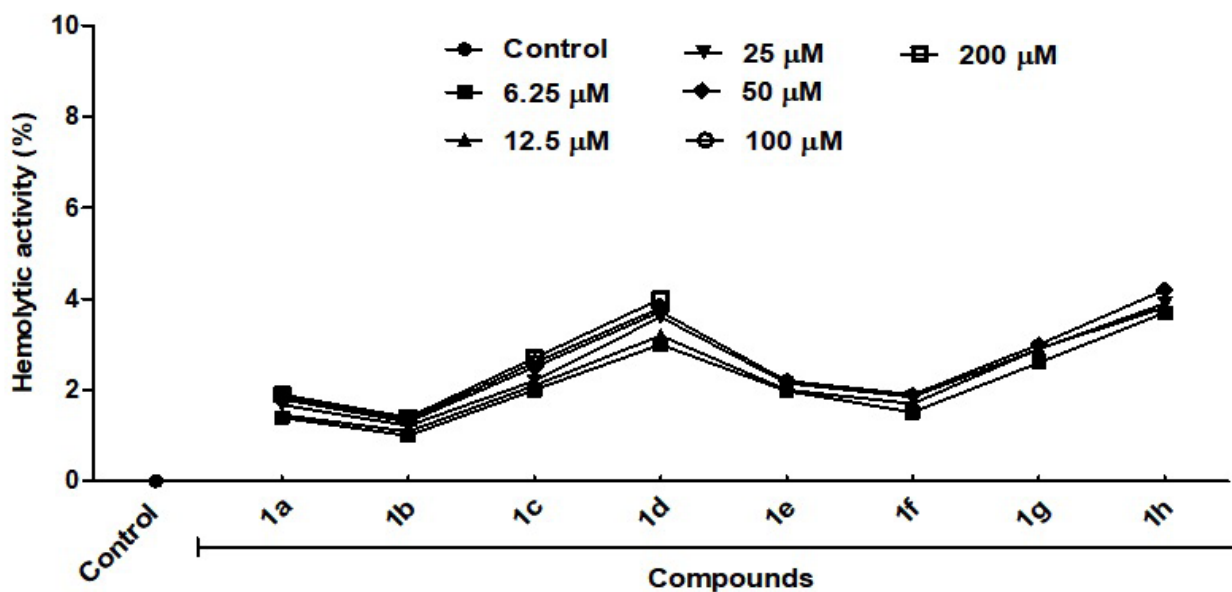


Figure 2. hemolytic activity results in different concentrations promoted by the compounds.

The results show that the compounds and standards (Miltefosine, Amphotericin B and Benznidazole) showed a percentage of hemolysis lower than 10% at the concentrations evaluated. Therefore, the compounds are not able to promote hemolysis *in vitro* (Amin & Dannenfelser 2006). The literature presents results of hemolytic activity for different thiazole derivatives. Sashidhara et al. (2015) evaluating chalcone-thiazole hybrids, Santana et al. (2018) evaluating thiazole compounds and Ansari et al. (2020) evaluating thiazol-2 (3H)-thiones containing the fraction 4-(3,4,5-trimethoxyphenyl) observed that they were not able to promote hemolysis in erythrocytes.

These findings reinforce that the compounds evaluated in our study are not considered hemolytic in *in vitro* assays. In addition to the hemolysis assays performed on erythrocytes, other mammalian cells were also evaluated in order to assess the cytotoxic

potential of the compounds. Table II presents the results of percentage of growth inhibition at a concentration of 200 μM and CC_{50} values for each of the compounds against the evaluated cells (RAW.264.7 macrophages, V79 fibroblasts and hepatoma (HepG2) cells).

The results show different IC_{50} results for the compounds. IC_{50} results for macrophage cells ranged from 45.12 to values greater than 200 μM . For fibroblast cells (V79) they ranged from 68.9 to greater than 200 μM , while for HepG2 cells they ranged from 73.4 to greater than 200 μM . Lower IC_{50} values indicate that the compounds are more toxic. Thus, we can highlight compounds 1b and 1d, the other compounds (1a, 1c, 1e, 1f, 1g and 1h) were not able to promote cytotoxicity in the different cells evaluated.

The literature presents different works evaluating different thiazole derivatives against mammalian cells. Rodrigues et al. (2018) evaluating the cytotoxic effect of 4-Phenyl-1,

Table II. Cytotoxicity results were expressed in percentage of growth inhibition at the highest concentration (200 μM) for the assays and in CC_{50} (capacity to inhibit growth by 50%) promoted by the compounds against RAW.264.7 macrophage cells, V79 fibroblasts and liver cells HepG2 respectively.

Compounds	Macrophages RAW.264.7 % Inhibition at 200 μM	Macrophages RAW.264.7 (CC_{50} μM)	Fibroblast (V79) % Inhibition at 200 μM	Fibroblast (V79) (CC_{50} μM)	Hepatoma (HepG2) % Inhibition at 200 μM	Hepatoma (HepG2) (CC_{50} μM)
1a	34.6 \pm 0.1	> 200	24.09 \pm 0.1	> 200	22.10 \pm 0.1	> 200
1b	100.0 \pm 10.0	45.12 \pm 0.12	88.98 \pm 1.0	68.9 \pm 0.3	84.99 \pm 0.1	73.4 \pm 0.1
1c	40.22 \pm 1.1	>200	29.92 \pm 0.1	> 200	31.01 \pm 0.1	> 200
1d	94.21 \pm 4.0	95.86 \pm 2.1	78.64 \pm 1.0	124.3 \pm 0.1	90.07 \pm 0.1	121.8 \pm 0.6
1e	45.30 \pm 0.1	> 200	11.05 \pm 0.1	> 200	43.86 \pm 1.0	> 200
1f	38.60 \pm 2.0	> 200	20.30 \pm 1.0	> 200	34.43 \pm 1.0	> 200
1g	26.46 \pm 1.1	> 200	20.13 \pm 0.1	> 200	22.66 \pm 0.1	> 200
1h	26.33 \pm 1.0	> 200	24.84 \pm 1.0	> 200	29.73 \pm 0.1	> 200
Miltefosine	99.5 \pm 0.1	7.1 \pm 0.2	38.78 \pm 0.5	> 200	83.23 \pm 2.0	125.70 \pm 0.3
Amphotericin B	99.8 \pm 0.0	15.57 \pm 0.03	27.35 \pm 0.9	> 200	85.67 \pm 1.5	150.90 \pm 0.1
Benznidazole	83.34 \pm 0.2	123.8 \pm 0.21	19.30 \pm 0.1	>200	35.23 \pm 1.0	>200

Mean \pm Standard Deviation.

3-thiazole-2-amines derivatives (8 compounds) against THP1, L929 and Vero cells, they obtained IC_{50} ranging from 45.73 to 143.57 μM , 27.07 to 198.26 μM and 118.17 to 1217.5 μM respectively, in addition, some compounds did not show toxicity. Teixeira et al. (2020) evaluating the cytotoxicity promoted by phthalimido-thiazole derivatives against RAW.264.7 macrophage cells obtained IC_{50} values that ranged from 59.7 to values greater than 413 μM . Gouveia et al. (2022) evaluating thiazolidine derivatives obtained IC_{50} values ranging from 8.52 to 126.83 μM against J774. A1 macrophages. Oliveira-Cardoso et al. (2014) obtained IC_{50} values for HepG2 cells ranging from 85.11 to 100 μM for 2-Pyridyl thiazoles compounds. Vra et al. (2019) obtained IC_{50} values for fibroblast cells from 12.01 to 209.53 μM for 4-thiazolidinone and 1,3-thiazole compounds.

These results reinforce that cytotoxicity is directly related to the chemical structure and cell type evaluated (Oliveira Cardoso et al. 2014, Rodrigues et al. 2018, Teixeira et al. 2020, Vra et al. 2019). Thus, the compounds evaluated in this study were able to promote moderate to low cytotoxicity against animal cells.

Evaluation of in vitro leishmanicidal activity

In vitro antipromastigote activity

Parasites of the *Leishmania* genus are digenetic (heteroxenes) and present in their life cycle only two evolutionary forms: the promastigote form, which is flagellated and extracellular, and the amastigote form, which is intracellular and without movements. Promastigotes have an elongated body, measuring between 14 and 20 μm and a free flagellum. Amastigotes have an ovoid body, measuring between 2.1 and 3.2 μm and an internal flagellum (Pessoa & Martins 1982).

To evaluate the leishmanicidal potential of the different compounds tested in the

promastigote forms of *L. amazonensis*, after 72 hours of treatment, the total number of promastigotes was counted under an optical microscope. Table III presents the results of the percentage of inhibition of growth of the promastigote forms at a concentration of 200 μM and IC_{50} values (concentration that inhibits the growth of the parasite by 50%) and the selectivity index between CC_{50} (mammal cells) and the IC_{50} (of the parasites) promoted by the compounds under study.

The compounds presented IC_{50} values that ranged from 19.86 to 200 μM and were classified according to scales adapted from the studies proposed by Upegui et al. (2014) and Gouveia et al. (2022) where compounds that presented $IC_{50} < 50 \mu\text{M}$ were considered active, those that presented IC_{50} between 50 and 200 μM moderately active and inactive with $IC_{50} > 200 \mu\text{M}$. Thus, compounds 1c, 1d, 1f, 1g and 1h were considered active and compound 1a moderately active and finally compounds 1b and 1e were considered inactive. The compounds when compared to Amphotericin B and Miltefosine showed low selectivity.

The literature reports the potential of thiazoles against promastigote forms. Rodrigues et al. (2018) evaluating 4-Phenyl-1,3-thiazol-2-amine derivatives against the promastigote form of *Leishmania amazonensis* obtained IC_{50} ranging from 20.78 to 957.56 μM . Haroon et al. (2021) evaluating 1,3-thiazole and 4-thiazolidinone ester derivatives against the promastigote form of *Leishmania infantum* obtained IC_{50} ranging from 14.39 to 374.16 μM and for the promastigote form of *Leishmania amazonensis* they obtained IC_{50} ranging from 13.35 to 484.67 μM , respectively.

The results presented showed that the compounds evaluated in this work are promising against the promastigote form of *Leishmania amazonensis* found in the sand fly (insect vector). However, even the compounds showing

Table III. Antipromastigote activity results obtained by the compounds expressed as percentage of inhibition at a concentration of 200 μM in addition to IC_{50} values and selectivity index.

Compounds	Promastigote % Inhibition at 200 μM	Promastigote (IC_{50} μM)	SI ($\text{CC}_{50}/\text{IC}_{50}$) ^a	SI ($\text{CC}_{50}/\text{IC}_{50}$) ^b	SI ($\text{CC}_{50}/\text{IC}_{50}$) ^c
1a	88.42 \pm 1.0	50.01	4.00	4.00	4.00
1b	19.77 \pm 0.8	>200	0.23	0.34	0.37
1c	88.43 \pm 1.1	19.86	10.07	10.07	10.07
1d	79.17 \pm 1.2	38.28	2.50	3.25	3.18
1e	37.89 \pm 0.1	>200	1.00	1.00	1.00
1f	92.40 \pm 1.0	24.33	8.22	8.22	8.22
1g	95.14 \pm 1.1	25.95	7.71	7.71	7.71
1h	98.76 \pm 0.9	32.58	6.14	6.14	6.14
Miltefosine	100	0.13	54.62	1538.46	966.92
Amphotericin B	100	0.83	18.76	240.96	181.81

Mean \pm Standard Deviation; SI: CC_{50} mammalian cells / IC_{50} promastigote; ^aMacrophages RAW.264.7; ^bFibroblast (V79); ^cHepatoma (HepG2). Selectivity results in absolute values.

potential, assays need to be carried out with the amastigote forms.

In vitro anti-amastigote activity

In addition to the promastigote forms, the cytotoxic effect of the compounds against the amastigote forms of *L. amazonensis*, after 72 hours of treatment, the viability was evaluated by optical microscope. Table IV presents the results of growth inhibition of intracellular amastigotes, IC_{50} values in addition to the selectivity and specificity indices in relation to macrophage cells.

The compounds presented IC_{50} values that ranged from 101 to greater than 200 μM and were also classified according to scales adapted from the studies proposed by Upegui et al. (2014) and Gouveia et al. (2022) previously used for the amastigote forms where compounds that presented $\text{IC}_{50} < 50$ μM were considered active, those that presented IC_{50} between 50 and 200 μM moderately active and inactive with $\text{IC}_{50} > 200$ μM . Thus, compounds 1a, 1c, 1d, 1e, 1f, 1g and 1h were considered moderately active, with very

close IC_{50} values, compound 1b was considered inactive.

The compounds showed low selectivity and compounds 1a, 1c, 1e, 1f, 1g and 1h were more toxic to the amastigote forms when compared to macrophage cells, that is, they showed lower IC_{50} values. Regarding specificity, compound 1e showed greater specificity, that is, it was more specific for the amastigote form. The others were more specific for the promastigote forms, with the exception of compound 1b, which did not show activity for any of the forms.

It is important to point out that the action on the amastigote form is hampered by the need for the compound to permeate through the macrophage membrane before reaching the parasite inside the cell, thus, there may be a loss of effectiveness of the compound for this form (Gouveia et al. 2022).

The literature presents different values of IC_{50} promoted for the thiazole compounds to different species of leishmania. Santos-Aliança et al. (2017) evaluating the leishmanicidal activity of phthalimido-thiazole derivatives obtained IC_{50}

Table IV. Results of anti-amastigote activity promoted by the compounds, percentage of inhibition of parasite growth at a concentration of 200 μ M, IC₅₀ values, selectivity and specificity index.

Compounds	Amastigote % Inhibition at 200 μ M	Amastigote (IC ₅₀ μ M)	SI (CC ₅₀ /IC ₅₀) ^a	SPI (IC ₅₀ /IC ₅₀) ^b
1a	55.3 \pm 1.0	101 \pm 0.2	1.98	0.50
1b	35.3 \pm 0.8	>200	0.23	1.00
1c	57.8 \pm 0.01	103 \pm 1.0	1.94	0.19
1d	60.2 \pm 0.02	102 \pm 0.01	0.94	0.38
1e	55.7 \pm 0.1	102 \pm 3.0	1.96	1.96
1f	53.3 \pm 1.0	101 \pm 2.1	1.98	0.24
1g	59.8 \pm 0.1	101 \pm 1.7	1.98	0.26
1h	69.9 \pm 0.02	102 \pm 1.1	1.96	0.32
Miltefosine	100	0.75 \pm 0.01	9.47	0.17
Amphotericin B	100	1.97 \pm 0.02	7.90	0.42

Mean \pm Standard Deviation; SI: CC₅₀ Macrophages RAW.264.7 /IC₅₀ amastigote; SPI: IC₅₀ promastigote /IC₅₀ amastigote. Selectivity and specificity results in absolute values.

values of 15.2 and 22.3 μ M. Queiroz et al. (2020) evaluating thiosemicarbazonic compounds and thiazoles observed that the compound GT-14 (a thiazole) was able to promote IC₅₀ of 16.51 μ M. Oliveira et al. (2020) obtained IC₅₀ ranging from 0.43 to 0.99 μ M.

The results found in the literature confirm that the compounds evaluated in this study promote moderate leishmanicidal activity against the amastigote forms of *Leishmania amazonensis*. Therefore, in order to choose the best compounds, cytotoxicity against mammalian cells and cytotoxicity against amastigote forms were evaluated. A compound with potential leishmanicidal activity must have low cytotoxicity against mammalian cells (high IC₅₀ values) and high cytotoxicity against the parasitic form (low IC₅₀ values). Thus, compounds 1a, 1c, 1e, 1f, 1g and 1h showed potential *in vitro* results against the amastigote forms.

Evaluation of cytotoxic activity against the forms of *Trypanosoma cruzi* *in vitro*

Cytotoxic activity against the trypomastigote form *in vitro*

The compounds were also evaluated against the trypomastigote form of *Trypanosoma cruzi*. Trypomastigote forms are elongated, with a kinetoplast with a rounded shape located in the region posterior to the nucleus, flagellum emerging from the flagellar pocket that is located laterally, in the posterior region of the parasite (Contreras et al. 2002, Takagi et al. 2022). The flagellum emerges and adheres along the body of the parasite, becoming free in the anterior region. This form is highly infectious, and can be found: in the insect vector; blood and intercellular space of vertebrate hosts I have macrophages as the main host (Contreras et al. 2002, Silva-Júnior et al. 2022, Takagi et al. 2022).

Table V presents the results of the percentage of inhibition of the growth of the trypomastigote forms at a concentration of 200

Table V. Antitrypomastigote activity results obtained by the compounds expressed as percentage of inhibition at a concentration of 200 μM in addition to IC_{50} values and selectivity index.

Compounds	Trypomastigote % Inhibition at 200 μM	Trypomastigote (IC_{50} μM)	SI ($\text{CC}_{50}/\text{IC}_{50}$) ^a	SI ($\text{CC}_{50}/\text{IC}_{50}$) ^b	SI ($\text{CC}_{50}/\text{IC}_{50}$) ^c
1a	58.7 \pm 0.1	100.0 \pm 1.2	2.00	2.00	2.00
1b	62.5 \pm 1.1	100.0 \pm 0.9	0.45	0.69	0.73
1c	90.60 \pm 0.1	2.50 \pm 0.01	80.00	80.00	80.00
1d	74.84 \pm 0.2	53.17 \pm 0.1	1.80	2.34	2.29
1e	99.0 \pm 0.02	1.72 \pm 0.02	116.28	116.28	116.28
1f	76.12 \pm 0.1	68.28 \pm 0.1	2.93	2.93	2.93
1g	61.61 \pm 0.02	100.0 \pm 1.1	2.00	2.00	2.00
1h	99.0 \pm 0.03	1.67 \pm 0.03	119.76	119.76	119.76
Benznidazole	99.0	14.60 \pm 0.1	8.48	13.70	13.70

Mean \pm Standard Deviation; SI: CC_{50} mammalian cells / IC_{50} trypomastigote; ^aMacrophages RAW.264.7; ^bFibroblast (V79); ^cHepatoma (HepG2). Selectivity results in absolute values.

μM and IC_{50} values (concentration that inhibits the growth of the parasite by 50%) and the selectivity index between CC_{50} (mammal cells) and the IC_{50} (of the parasites) promoted by the compounds under study.

The results presented in the Table V show that the compounds presented IC_{50} ranging from 1.67 to 100 μM . Compounds 1c, 1e and 1h were considered active and presented IC_{50} values lower than the standard benznidazole. Furthermore, the compounds in ascending order 1c, 1e and 1h showed a high selectivity index, that is, they were more selective for the trypomastigote forms when compared to mammalian cells. The other compounds (1a, 1b, 1d, 1f and 1g) were considered moderately active.

The thiazoles show promising activity against the trypomastigote forms. Among the different studies, we can mention those carried out by Gomes et al. (2016) evaluating Phthalimido-thiazoles compounds against trypomastigote forms of *Trypanosoma cruzi* obtained IC_{50} values ranging from 0.5 to 107.5 μM . Oliveira-Cardoso et al. (2014) obtained IC_{50} values ranging from 1.1 to 36.7 μM for the 2-Pyridyl thiazoles compounds.

Silva et al. (2017) obtained IC_{50} values ranging from 1.2 to 13.0 μM for the compounds 2-(pyridin-2-yl)-1,3-thiazoles. Vra et al. (2019) obtained IC_{50} values ranging from 9.65 to 169.66 μM for 4-thiazolidinone and 1,3-thiazole compounds. Oliveira-Filho et al. (2017) evaluating different thiazoles obtained IC_{50} values ranging from 0.37 to values greater than 50 μM .

These results show that compounds 1c, 1e and 1f show promising activity against the trypomastigote forms of *Trypanosoma cruzi*.

Cytotoxic activity against the amastigote form *in vitro*

The compounds were also evaluated against the amastigote form of *Trypanosoma cruzi*. The results of anti-amastigote activity are shown in Table VI.

The results presented in Table VI show that the compounds showed anti-amastigote activity ranging from 1.96 to values greater than 200 μM . Compounds 1c, 1e and 1g were considered active, in addition, they showed the highest levels of selectivity. Compounds 1d and 1f moderately active and the others inactive.

Table VI. Antiamastigote activity results obtained by the compounds expressed as percentage of inhibition at a concentration of 200 μM in addition to IC_{50} values and selectivity index.

Compounds	Amastigote % Inhibition at 200 μM	Amastigote (IC_{50} μM)	SI ($\text{CC}_{50}/\text{IC}_{50}$)	SPI ($\text{IC}_{50}/\text{IC}_{50}$)
1a	19.77 \pm 0.1	>200	1.00	0.50
1b	22.66 \pm 0.2	>200	0.23	0.50
1c	99.85 \pm 0.11	6.12 \pm 0.1	32.68	0.41
1d	69.96 \pm 0.3	62.82 \pm 1.0	1.53	0.85
1e	99.89 \pm 1.0	1.96 \pm 0.01	102.04	0.88
1f	74.13 \pm 0.11	84.97 \pm 1.1	2.35	0.80
1g	61.61 \pm 0.12	2.46 \pm 0.2	81.30	40.65
1h	99.89 \pm 1.5	>200	1.00	0.01
Beznidazole	100	5.65 \pm 0.01	21.91	2.58

Mean \pm Standard Deviation; SI: CC_{50} Macrophages RAW.264.7 / IC_{50} amastigote; SPI: IC_{50} promastigote / IC_{50} amastigote. Selectivity and specificity results in absolute values.

Regarding specificity, only compound 1g showed greater specificity against the amastigote form when compared to the trypomastigote form.

The literature reports that thiazoles are compounds with potential anti-amastigote activity. Vra et al. (2019) obtained IC_{50} values ranging from 5.28 to 52.99 μM for 4-thiazolidinone and 1,3-thiazole compounds. Álvarez et al. (2015a) evaluating the activity of a thiazole containing an amide group against the amastigote form, they obtained an IC_{50} of 0.72 μM . Álvarez et al. (2015b) evaluating the activity of a bis-thiazole compound, they obtained IC_{50} results of 1.2 μM . Haroon et al. (2021) obtained IC_{50} values for the amastigote forms ranging from 16.85 to 75.39 μM .

The results found in the literature show that the compounds evaluated in this work showed promising results against the amastigote form of *Trypanosoma cruzi*. Therefore, the choice of the best compounds against the forms of *Trypanosoma cruzi* was carried out. Trypomastigote and amastigote forms are found in the vertebrate host. With this, the selection

proceeded on compounds that presented low cytotoxicity against animal cells (high IC_{50}) and high cytotoxicity (low IC_{50}) against the trypomastigote and amastigote forms. The selected compounds were compounds 1c and 1e effective for both forms of the parasite. Again, it was observed that for the amastigote form, an increase in concentration when compared to the trypomastigote form, this is because, for the compound to promote activity, it is necessary that its cross different membranes until it reaches the parasite that is intracellular (Gouveia et al. 2022).

CONCLUSIONS

This study presented a screening to verify the biological potential of eight thiazole compounds. The study showed that they had good pharmacokinetic profiles, moderate to low antioxidant activity. In addition, they also have moderate to low cytotoxicity. Antiparasitic assays for *Leishmania amazonensis* and *Trypanosoma cruzi* *in vitro* show promising results, with

emphasis on compounds 1c for leishmanicidal activity and 1e for trypanocidal activity, which, in addition to presenting low toxicity against mammalian cells. Therefore, this study generally showed that the compounds evaluated may be good candidates for antiparasitic drugs.

Acknowledgments

This study was supported by the Fundação de Amparo a Ciência e Tecnologia de Pernambuco (FACEPE, Process APQ-0498-4.03/19), Research Scholarship - FACEPE (Process BFP-0038-04.03/21) and Scholarship from the Conselho Nacional de Desenvolvimento Científico e Tecnológico (CNPq, Process 306865/612020-3).

REFERENCES

- AHMED A, AUNE D, VINEIS P, PESCARINI JM, MILLETT C & HONE T. 2022. The effect of conditional cash transfers on the control of neglected tropical disease: a systematic review. *Lancet Glob Health*10(5): e640-e648. doi.org/10.1016/S2214-109X(22)00065-1.
- ÁLVAREZ G ET AL. 2015a. Identification of a new amide-containing thiazole as a drug candidate for treatment of Chagas' disease. *Antimicrob Agents Chemother* 59(3): 1398-1404. doi.org/10.1128/AAC.03814-14.
- ÁLVAREZ G ET AL. 2015b. Development of bis-thiazoles as inhibitors of triosephosphate isomerase from *Trypanosoma cruzi*. Identification of new non-mutagenic agents that are active in vivo. *Eur J Med Chem* 100: 246-256. doi.org/10.1016/j.ejmech.2015.06.018.
- ALVES JEF, OLIVEIRA JF, LIMA SOUZA TRC, MOURA RO, CARVALHO JUNIOR LB, LIMA MDCA & ALMEIDA SMV. 2021. Novel indole-thiazole and indole-thiazolidinone derivatives as DNA groove binders. *Int J Biol Macromol* 170: 622-635. doi.org/10.1016/j.ijbiomac.2020.12.153.
- AMIN K & DANNENFELSER RM. 2006. In vitro hemolysis: guidance for the pharmaceutical scientist. *J Pharm Sci* 95(6): 1173-1176. doi.org/10.1002/jps.20627.
- ANDREANI A ET AL. 2013. Chemopreventive and antioxidant activity of 6-substituted imidazo [2, 1-b] thiazoles. *Eur J Med Chem* 68: 412-421. doi.org/10.1016/j.ejmech.2013.07.052.
- ANSARI M, SHOKRZADEH M, KARIMA S, RAJAEI S, FALLAH M, GHASSEMI-BARGHI N & EMAMI S. 2020. New thiazole-2 (3H)-thiones containing 4-(3, 4, 5-trimethoxyphenyl) moiety as anticancer agents. *Eur J Med Chem* 185: 111784. doi.org/10.1016/j.ejmech.2019.111784.
- BILEN E, ÖZMEN ÜÖ, ÇETE S, ALYAR S & YAŞAR A. 2022. Bioactive sulfonyl hydrazones with alkyl derivative: Characterization, ADME properties, molecular docking studies and investigation of inhibition of choline esterase enzymes for the diagnosis of Alzheimer's disease. *Chem Biol Interact* 360: 109956. doi.org/10.1016/j.cbi.2022.109956.
- CHANDA K. 2021. An Overview on the Therapeutics of Neglected Infectious Diseases—Leishmaniasis and Chagas Diseases. *Front Chem* 9: 37. doi.org/10.3389/fchem.2021.622286.
- CHHABRIA M, PATEL S, MODI P & BRAHMKSHATRIYA P. 2016. Thiazole: A review on chemistry, synthesis and therapeutic importance of its derivatives. *Curr Top Med Chem* 16(26): 2841-2862.
- CONTRERAS VT, NAVARRO, MC, LIMA AR, ARTEAGA R, DURAN F, ASKUE J & FRANCO Y. 2002. Production of amastigotes from metacyclic trypomastigotes of *Trypanosoma cruzi*. *Mem Inst Oswaldo Cruz* 97(8): 1213-1220.
- DINCEL ED, GÜRISOY E, YILMAZ-OZDEN T & ULUSOY-GÜZELDEMIRCI N. 2020. Antioxidant activity of novel imidazo [2, 1-b] thiazole derivatives: Design, synthesis, biological evaluation, molecular docking study and in silico ADME prediction. *Bioorg Chem* 103: 104220. doi.org/10.1016/j.bioorg.2020.104220.
- DOMÍNGUEZ-VILLA FX, DURÁN-ITURBIDE NA & ÁVILA-ZÁRRAGA JG. 2021. Synthesis, molecular docking, and in silico ADME/Tox profiling studies of new 1-aryl-5-(3-azidopropyl) indol-4-ones: Potential inhibitors of SARS CoV-2 main protease. *Bioorg Chem* 106: 104497. doi.org/10.1016/j.bioorg.2020.104497.
- EL-ACHKAR GA ET AL. 2015. Thiazole derivatives as inhibitors of cyclooxygenases in vitro and in vivo. *Eur J Pharmacol* 750: 66-73. doi.org/10.1016/j.ejphar.2015.01.008.
- ELPHICK-POOLEY T & ENGELS D. 2022. World NTD Day 2022 and a new Kigali Declaration to galvanise commitment to end neglected tropical diseases. *Infect Dis Poverty* 11(1): 1-3. doi.org/10.1186/s40249-021-00932-2.
- FOWLER S ET AL. 2022. Addressing Today's Absorption, Distribution, Metabolism, and Excretion (ADME) Challenges in the Translation of In Vitro ADME Characteristics to Humans: A Case Study of the SMN2 mRNA Splicing Modifier Risdiplam. *Drug Meta Dispos* 50(1): 65-75. doi.org/10.1124/dmd.121.000563.
- GOMES PAT ET AL. 2016. Phthalimido-thiazoles as building blocks and their effects on the growth and morphology

- of *Trypanosoma cruzi*. *Eur J Med Chem* 111: 46-57. doi.org/10.1016/j.ejmech.2016.01.010.
- GONZÁLEZ DLN, CASTAÑO JAG, NÚÑEZ WER & DUCHOWICZ PR. 2021. Antiprotozoal QSAR modelling for trypanosomiasis (Chagas disease) based on thiosemicarbazone and thiazole derivatives. *J Mol Graph Model* 103: 107821. doi.org/10.1016/j.jmgm.2020.107821.
- GOUEIA AL ET AL. 2022. Thiazolidine derivatives: In vitro toxicity assessment against promastigote and amastigote forms of *Leishmania infantum* and ultrastructural study. *Exp Parasitol* 236: 108253. doi.org/10.1016/j.exppara.2022.108253.
- HAROON M ET AL. 2021. The design, synthesis, and in vitro trypanocidal and leishmanicidal activities of 1,3-thiazole and 4-thiazolidinone ester derivatives. *RSC Adv* 11(4): 2487-2500. doi.org/10.1039/D0RA06994A.
- JACOB ÍT ET AL. 2021. Anti-inflammatory activity of novel thiosemicarbazone compounds indole-based as COX inhibitors. *Pharmacol Rep* 73(3): 907-925. doi.org/10.1007/s43440-021-00221-7.
- KHAMEES HA ET AL. 2019. Molecular structure, DFT, vibrational spectra with fluorescence effect, hirshfeld surface, docking simulation and antioxidant activity of thiazole derivative. *ChemistrySelect* 4(15): 4544-4558. doi.org/10.1002/slct.201900646.
- LIUS & SHAH DK. 2022. Mathematical models to characterize the absorption, distribution, metabolism, and excretion (ADME) of protein therapeutics. *Drug Metab Dispos* 50(6) doi.org/10.1124/dmd.121.000460.
- MARQUES-GARCIA F. 2020. Methods for hemolysis interference study in laboratory medicine—a critical review. *Ejifcc* 31(1): 85.
- MARTÍNEZ-CERÓN S, GUTIÉRREZ-NÁGERA NA, MIRZAEICHESHMEH E, CUEVAS-HERNÁNDEZ RI & TRUJILLO-FERRARA JG. 2021. Phenylbenzothiazole derivatives: effects against a *Trypanosoma cruzi* infection and toxicological profiles. *Parasitol Res* 120(8): 2905-2918. doi.org/10.1007/s00436-021-07137-4.
- MOHARRAM HA & YOUSSEF MM. 2014. Methods for determining the antioxidant activity: a review. *Alex J Food Sci Tech* 11(1): 31-42.
- NAQVI FA, DASJK, SALAM RA, RAZA SF, LASSI ZS & BHUTTA ZA. 2022. Interventions for neglected tropical diseases among children and adolescents: a meta-analysis. *Pediatrics* 149(Supplement 6): doi.org/10.1542/peds.2021-053852E.
- NORINDER U & BERGSTRÖM CA. 2006. Prediction of ADMET properties. *ChemMedChem* 1(9): 920-937. doi.org/10.1002/cmdc.200600155.
- OLIVEIRA CARDOSO MV ET AL. 2014. 2-Pyridyl thiazoles as novel anti-*Trypanosoma cruzi* agents: Structural design, synthesis and pharmacological evaluation. *Eur J Med Chem* 86: 48-59. doi.org/10.1016/j.ejmech.2014.08.012.
- OLIVEIRA FILHO GB ET AL. 2017. Structural design, synthesis and pharmacological evaluation of thiazoles against *Trypanosoma cruzi*. *Eur J Med Chem* 141: 346-361.
- OLIVEIRA JF ET AL. 2015. Synthesis of thiophene-thiosemicarbazone derivatives and evaluation of their in vitro and in vivo antitumor activities. *Eur J Med Chem* 104: 148-156. doi.org/10.1016/j.ejmech.2015.09.036.
- OLIVEIRA VVG, SOUZA MAA, CAVALCANTI RRM, OLIVEIRA CARDOSO, MV, LEITE ACL, SILVA JUNIOR, VA & FIGUEIREDO RCBQ. 2020. Study of in vitro biological activity of thiazoles on *Leishmania (Leishmania) infantum*. *J Glob Antimicrob Resist* 22: 414-421. doi.org/10.1016/j.jgar.2020.02.028.
- OTTE J & PICA-CIAMARRA U. 2021. Emerging infectious zoonotic diseases: The neglected role of food animals. *One Health* 13: 100323. doi.org/10.1016/j.onehlt.2021.100323.
- PALANIMUTHU D & SAMUELSON AG. 2013. Dinuclear zinc bis (thiosemicarbazone) complexes: Synthesis, in vitro anticancer activity, cellular uptake and DNA interaction study. *Inorganica Chim Acta* 408: 152-161. doi.org/10.1016/j.ica.2013.09.014.
- PERDOMO C ET AL. 2021. Preclinical Studies in Anti-Trypanosomatidae. *Drug Dev Ind Pharm* 14(7): 644. doi.org/10.3390/ph14070644.
- PESSOA SB & MARTINS AV. 1982. *Parasitologia Médica*. 115ª ed., Rio de Janeiro, p. 838.
- PETROU A, FESATIDOU M & GERONIKAKI A. 2021. Thiazole ring—A biologically active scaffold. *Molecules* 26(11): 3166. doi.org/10.3390/molecules26113166.
- PIRES DE, BLUNDELL TL & ASCHER DB. 2015. pkCSM: predicting small-molecule pharmacokinetic and toxicity properties using graph-based signatures. *J Med Chem* 58(9): 4066-4072. doi.org/10.1021/acs.jmedchem.5b00104.
- QUEIROZ CM ET AL. 2020. Thiosemicarbazone and thiazole: in vitro evaluation of leishmanicidal and ultrastructural activity on *Leishmania infantum*. *Med Chem Res* 29(11): 2050-2065.
- RODRIGUES CA ET AL. 2018. 4-Phenyl-1, 3-thiazole-2-amines as scaffolds for new antileishmanial agents. *J Venom Anim Toxins Incl Trop Dis* 24: doi.org/10.1186/s40409-018-0163-x.
- RUIZ R ET AL. 2010. Biological assays and noncovalent interactions of pyridine-2-carbaldehyde

thiosemicarbazonecopper (II) drugs with [poly (dA–dT)]₂, [poly (dG–dC)]₂, and calf thymus DNA. *JBIC* 15(4): 515–532. doi.org/10.1007/s00775-009-0620-7.

SALAR U ET AL. 2017. New hybrid hydrazinyl thiazole substituted chromones: As potential α -amylase inhibitors and radical (DPPH & ABTS) scavengers. *Sci Rep* 7(1): 1–17. doi.org/10.1038/s41598-017-17261-w.

SAMALA G, DEVI PB, SAXENA S, MEDA N, YOGESHWARI P & SRIRAM D. 2016. Design, synthesis and biological evaluation of imidazo [2, 1-b] thiazole and benzo [d] imidazo [2, 1-b] thiazole derivatives as Mycobacterium tuberculosis pantothenate synthetase inhibitors. *Bioorg Med Chem* 24(6): 1298–1307. doi.org/10.1016/j.bmc.2016.01.059.

SANTANA TI, OLIVEIRA BARBOSA M, MORAES GOMES PAT, CRUZ ACN, SILVA TG & LEITE ACL. 2018. Synthesis, anticancer activity and mechanism of action of new thiazole derivatives. *Eur J Med Chem* 144: 874–886.

SANTOS ALIANÇA AS ET AL. 2017. In vitro evaluation of cytotoxicity and leishmanicidal activity of phthalimido-thiazole derivatives. *Eur J Pharm Sci* 105: 1–10. doi.org/10.1016/j.ejps.2017.05.005.

SANTOS SS, ARAUJO RV, GIAROLLA J, EL SEOUD O & FERREIRA EI. 2020. Searching for drugs for Chagas disease, leishmaniasis and schistosomiasis: a review. *Int J Antimicrob Agents* 55(4): 105906. doi.org/10.1016/j.ijantimicag.2020.105906.

SASHIDHARA KV ET AL. 2015. Novel chalcone–thiazole hybrids as potent inhibitors of drug resistant Staphylococcus aureus. *ACS* 6(7): 809–813. doi.org/10.1021/acsmedchemlett.5b00169.

SCARIM CB, JORNADA DH, MACHADO MGM, FERREIRA CMR, SANTOS JL & CHUNG MC. 2019. Thiazole, thio and semicarbazone derivatives against tropical infective diseases: Chagas disease, human African trypanosomiasis (HAT), leishmaniasis, and malaria. *Eur J Med Chem* 162: 378–395. doi.org/10.1016/j.ejmech.2018.11.013.

SHALABY EA & SHANAB SM. 2013. Antioxidant compounds, assays of determination and mode of action. *Afr J Pharm Pharmacol* 7(10): 528–539. doi.org/10.5897/AJPP2013.3474.

SILVA EB, SILVA DAO, OLIVEIRA AR, SILVA MENDES CH, DOS SANTOS TAR, SILVA AC & LEITE ACL. 2017. Design and synthesis of potent anti-Trypanosoma cruzi agents new thiazoles derivatives which induce apoptotic parasite death. *Eur J Med Chem* 130: 39–50. doi.org/10.1016/j.ejmech.2017.02.026.

SILVA JÚNIOR JN ET AL. 2022. Do thiazolidine compounds act on intracellular amastigotes of Trypanosoma cruzi? A systematic review. *Res Soc Dev* 11(3):

e38611326531–e3861132653. doi.org/10.33448/rsd-v11i3.26531.

SILVA PR ET AL. 2020. Novel indol-3-yl-thiosemicarbazone derivatives: Obtaining, evaluation of in vitro leishmanicidal activity and ultrastructural studies. *Chem Biol Interact* 315: 108899. doi.org/10.1016/j.cbi.2019.108899.

SOUZA AA ET AL. 2021. Diagnostics and the neglected tropical diseases roadmap: setting the agenda for 2030. *Trans R Soc Trop Med Hyg* 115(2):129–135. doi.org/10.1093/trstmh/traa118.

TABTI K, BAAMMI S, ELMCHICHI L, SBAI A, MAGHAT H, BOUACHRINE M & LAKHLIFI T. 2022. Computational investigation of pyrrolidin derivatives as novel GPX4/MDM2–p53 inhibitors using 2D/3D-QSAR, ADME/toxicity, molecular docking, molecular dynamics simulations, and MM-GBSA free energy. *Struct Chem* 33(4): 1019–1039. doi.org/10.1007/s11224-022-01903-5.

TAKAGI Y, SATO M, NAYA M & SATO C. 2022. Differentiating Trypanosoma cruzi in a Host Mammalian Cell Imaged in Aqueous Liquid by Atmospheric Scanning Electron Microscopy. *Microbiol Spectr* 10(1): e01413–21. doi.org/10.1128/spectrum.01413-21.

TEIXEIRA MGPA ET AL. 2020. Dual Parasiticidal Activities of Phthalimides: Synthesis and Biological Profile against Trypanosoma cruzi and Plasmodium falciparum. *ChemMedChem* 15(22): 2164–2175. doi.org/10.1002/cmdc.202000331.

UPEGUI Y, GIL JF, QUIÑONES W, TORRES F, ESCOBAR G, ROBLEDO SM & ECHEVERRI F. 2014. Preparation of rotenone derivatives and in vitro analysis of their antimalarial, antileishmanial and selective cytotoxic activities. *Molecules* 19(11): 18911–18922. doi.org/10.3390/molecules191118911.

VRA DSSA, JÚNIOR PAS, ROMANHA AJ & LEITE ACL. 2019. Synthesis and anti-Trypanosoma cruzi profile of the novel 4-thiazolidinone and 1,3-thiazole derivatives. *Front Drug Chem Clin* 2: 1–12. doi.org/10.15761/FDCCR.1000120.

ZHOU XN. 2022. Infectious Diseases of Poverty: progress achieved during the decade gone and perspectives for the future. *Infect Dis Poverty* 11(1): 1–4. doi.org/10.1186/s40249-021-00931-3.

SUPPLEMENTARY MATERIAL

Table S1.

Figure S1.

How to cite

CRUZ FILHO IJ, OLIVEIRA JF, SANTOS ACS, PEREIRA VRA & LIMA MCA. 2023. Synthesis of 4-(4-chlorophenyl)thiazole compounds: *in silico* and *in vitro* evaluations as leishmanicidal and trypanocidal agents. *An Acad Bras Cienc* 95: e20220538. DOI 10.1590/0001-3765202320220538.

*Manuscript received on June 28, 2022;
accepted for publication on February 23, 2023*

IRANILDO JOSÉ DA CRUZ FILHO¹

<https://orcid.org/0000-0002-5466-6567>

JAMERSON F. DE OLIVEIRA²

<https://orcid.org/0000-0001-9606-8154>

ALINE CAROLINE S. SANTOS³

<https://orcid.org/0000-0002-8592-395X>

VALÉRIA R.A. PEREIRA³

<https://orcid.org/0000-0002-7995-7360>

MARIA CARMO A. DE LIMA¹

<https://orcid.org/0000-0002-8277-3458>

¹Federal University of Pernambuco (UFPE), Department of Antibiotics, Av. Prof. Moraes Rego, 1235, Cidade Universitária, 50670-901 Recife, PE, Brazil

²University of International Integration of Afro-Brazilian Lusophony (UNILAB), Av. da Abolição, 3, Centro 62790-970 Redenção, CE, Brazil

³Oswaldo Cruz Pernambuco Foundation (Fiocruz/PE), Department of Immunology, Av. Prof. Moraes Rego, 1235, Cidade Universitária 50670-901 Recife, PE, Brazil

Correspondence to: **Iranildo José da Cruz Filho**

E-mail: iranildoj@gmail.com

Author contributions

Iranildo José da Cruz Filho: Conceptualization, Investigation, Methodology, Validation, Formal analysis, Writing - Original Draft, Writing - Review & Editing. Jamerson Ferreira de Oliveira: Conceptualization, Investigation, Methodology, Validation, Formal analysis, Writing - Original Draft, Writing - Review & Editing. Aline Caroline da Silva Santos: Conceptualization, Investigation, Methodology, Validation, Formal analysis, Writing - Original Draft, Writing - Review & Editing. Valéria Rêgo Alves Pereira: Conceptualization, Methodology, Formal analysis, Resources, Writing - Original Draft, Writing - Review & Editing, Supervision, Project administration. Maria do Carmo Alves de Lima: Conceptualization, Investigation, Methodology, Validation, Formal analysis, Writing - Original Draft, Writing - Review & Editing; Conceptualization, Methodology, Formal analysis, Resources, Writing - Original Draft, Writing - Review & Editing, Supervision, Project administration.

